Ferricytochrome b5: assignment of heme propionate resonances on the basis of nuclear Overhauser effect measurements and the nature of interprotein contacts with partner redox prote...

ARTICLE *in* JOURNAL OF THE AMERICAN CHEMICAL SOCIETY · MARCH 1986

Impact Factor: 12.11 · DOI: 10.1021/ja00266a026

3 AUTHORS, INCLUDING:

Einar Sletten
University of Bergen
107 PUBLICATIONS **1,913** CITATIONS

SEE PROFILE

leaving amide II′ at ~1460 cm^{-1} as a nearly pure C–N stretching mode. Amides I, II, and III are all seen in UVRR spectra excited near the amide absorption band.[8-12,15-17] The strongest of the three is amide II; amide II′ is even stronger, becoming the dominant feature of the UVRR protein spectra run in D_2O (see Figure 2). Moreover, the molar scattering factors for amide II′ are close to the sums of those for amides II and III (see Table II). As discussed by Hudson and co-workers,[11,17] this behavior implies that C–N stretching is the main distortion coordinate for the amide π–π^* excited state, which has a particularly large Franck–Condon factor for amides II and II′.

This interpretation is fully in accord with the observed Raman hypochromism, which affects the amide II, II′, and III bands. Indeed the Raman intensities of these bands do scale roughly with the square of the absorption strength, as expected. Thus, Rosenheck and Doty have measured molar absorptivities for α-helical and random coil peptides of 4100 and 6900 at 190 nm.[18] The ratio of their squares, 2.83, compares well with the ratios of the molar scattering factors for amides II, II′, and III, 2.15, 3.32, and 1.96, respectively. It can be inferred that these bands gain nearly all their intensity from resonance with the 190-nm π–π^* transition. This is also the conclusion of Dudik et al.,[12] who found that the preresonance excitation profiles for the amide II and III bands of acetamide and *N*-methylacetamide could be accurately fit by *A* term (Franck–Condon) scattering via the π–π^* transitions. With visible wavelength excitation, far from resonance, the amide III band is weak but still shows preresonant hypochromism for α-helical peptides,[20,33] while amide II is too weak to be observed. On the other hand, the amide I band is a strong feature of the visible Raman spectra, and the near invariance of its intensity with α-helical content implies that it gains very little of its intensity from the 190-nm electronic transition. In the visible region, it actually shows increased strength for α-helices, and Painter and Koenig[33] have suggested enhancement via the n–π^* transition at ~220 nm, which is somewhat augmented for α-helices. This transition is very weak ($\epsilon \sim 100$),[40] however, and probably does not contribute significantly to the amide I intensity at 200 nm, which no doubt derives mainly from higher lying excited states which are known to be hyperchromic for α-helical polypeptides.[38] Dudik et al.[12] found no evidence for enhancement of the C=O stretching mode of acetone, analogous to the amide I mode of peptides, at excitation wavelengths within the weak, isolated n–π^* absorption band at 215 nm.

Tropomyosin was chosen for this study because it exists in only two conformations, α-helix and random coil,[41] whose fractions can be varied over a wide range by adjusting the pH.[19] In analyzing other proteins, one must consider the possibility that the molar scattering factors may have a range of values for different peptide conformations. The absorption studies of Rosenheck and Doty[18] showed that the amide absorptivity is slightly higher but nearly the same for β-sheet peptides as for the random coil. We expect the difference between the random coil and β-sheet peptides to be likewise small in the UV Raman spectrum, the β-sheet form perhaps showing slight *hyper*chromism. Thus, hypochromism appears to be a unique characteristic of the α-helix. In this case, the molar scattering factors may have one set of values for α-helical peptides and a narrow range of values for all other conformations. This assumption is implicit in our use of the UVRR intensities to estimate the α-helical content of myoglobin, cytochrome *c*, and bovine serum albumin. These proteins span a wide range of helix contents, and the good agreement with other methods, particularly X-ray crystallography (Table III), suggests that the assumption may be reasonable. It therefore appears that the UVRR technique may offer a sensitive and relatively interference-free method for helix content determination in polypeptides and proteins.

Acknowledgment. This work was supported by NSF Grant CHE 8106084 and NIH Grant GM 25158.

Note Added in Proof. While this paper was under review, Chinsky et al.[42] reported preresonance Raman spectra of poly(L-lysine) in its α-helix and random coil forms and native and denatured (80 °C) ribonuclease A with 248-nm excitation. Although the authors make no mention of it, their data show clear evidence of hypochromism for the amide II and III modes associated with the α-helix secondary structure (see Figures 2 and 7 of ref 42).

(40) Cantor, C. R.; Schimmel, P. R. "Biophysical Chemistry"; W. H. Freeman: San Francisco, 1980; Part II, pp 375.

(41) Talbot, J. A.; Hodges, R. S. *Acc. Chem. Res.* **1982**, *15*, 224–230.

(42) Chinsky, L.; Jolles, B.; Laigle, A.; Turpin, P. Y. *J. Raman Spectrosc.* **1985**, *16*, 235–241.

Ferricytochrome b_5: Assignment of Heme Propionate Resonances on the Basis of Nuclear Overhauser Effect Measurements and the Nature of Interprotein Contacts with Partner Redox Proteins

Stuart J. McLachlan,[1a] Gerd N. La Mar,*[1a] and Einar Sletten[1b]

Contribution from the Departments of Chemistry, University of California, Davis, California 95616, and University of Bergen, Bergen, Norway. *Received August 5, 1985*

Abstract: Nuclear Overhauser effect experiments have lead to the stereospecific assignment of the four methylene proton pairs of the heme propionate side chains in ferricytochrome b_5. The pH-sensitive resonances have been assigned to the exposed heme propionate on the heme pyrrole ring III. In addition it has been shown that this group is able to bind extrinsic metal ions and is intimately involved in the binding site for redox partner proteins. The patterns of the α-methylene proton hyperfine shifts for both propionates are concluded to be inconsistent with the orientation obtained from available X-ray crystal coordinates and suggest specific rotations for each side chain. The nature of the slight changes resulting from complex formation with partner redox proteins such as cytochrome *c* or myoglobin is shown to be consistent with a decrease of the p*K* for the exposed 6-propionate carboxylate. This decrease supports a direct participation of this group in a salt bridge to the partner protein.

Cytochrome b_5 is found both as a membrane-bound protein in mammalian liver microsomes as well as a soluble form in erythrocytes. The microsomal protein plays an important role in fatty acid desaturation[2] while the soluble form acts as an electron

0002-7863/86/1508-1285$01.50/0

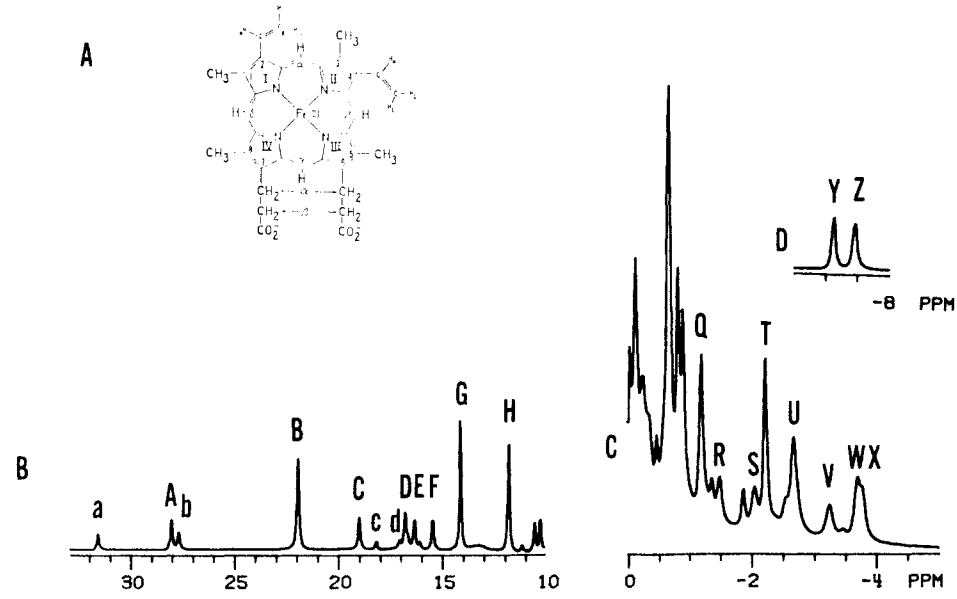

Figure 1. (A) Structure of the heme group found in ferricytochrome b_5. (B–D) Resolved portions of the hyperfine-shifted region of the 500-MHz ^1H NMR spectrum of ferricytochrome b_5 at pH 6.2 and 20 °C in ^2H_2O.

mediator in the erythrocyte methemoglobin reductase system.[3] Microsomal cytochrome b_5 and an outer mitochondrial membrane cytochrome b have both been detected in heart muscle by the use of immunological methods.[4] Their presence suggests that cytochrome b_5 may be involved in the muscle metmyoglobin reductase system.[5,6] The trypsin-solubilized fragment of cytochrome b_5 from bovine liver microsomes contains the heme prosthetic group (A in Figure 1) and consists of 84 amino acids. This solubilized fragment has been extensively studied and has been shown to retain full activity.[7] This solubilized fragment, moreover, exhibits essentially the same spectral characteristics and properties as the soluble erythrocyte protein.[8] The structure of the lipase-solubilized fragment of cytochrome b_5 has been solved by X-ray diffraction for both the reduced and oxidized states.[9,10] The lipase fragment contains amino acid residues 1–93 and is a good model for the trypsin fragment containing residues 3–86.

The trypsin-solubilized ferricytochrome b_5 fragment has been reported to form 1:1 solution complexes with cytochrome c,[11,12] myoglobin,[6] and hemoglobin.[13] In the former two complexes,[12,6] the binding is clearly detected by ^1H NMR by highly selective perturbations of a small number of resonances. Previous studies have suggested that the pH- and complex-formation-sensitive resonances originate in the heme propionate,[14,15] but experimental vertification is lacking. The special role of the heme propionates in cytochrome b_5 function has been emphasized in several studies. The computer "docking" of partner redox proteins based on charge complementarity has invoked an interprotein salt bridge for the exposed 6-propionate side chain.[16,17] Moreover, the unusual interaction of a small cation with the buried 7-propionate carboxylate group has been suggested to play a role in stabilizing the reduced protein.[9] The confirmation of these specific roles for heme propionates on the basis of ^1H NMR spectral properties first requires the unambiguous assignments. The analysis of the nature of the propionate side chain hyperfine shifts and their sensitivity to complex formation may shed light on the mode of protein–protein interaction.

To date, ^1H NMR spectral assignments in ferricytochromes have relied on two methods, nuclear Overhauser effect (NOE) based assignments on the diamagnetic, reduced protein followed by connectivities to the ferric form by saturation transfer via electron exchange[18,19] and by direct reconstitution with isotope-labeled hemes.[20,21] The two methods have provided the location and assignment of the signals in ferricytochrome b_5 for all four heme methyl groups, the 2-vinyl group, two of the four propionate β-methylene protons, and a few amino acid side chains in the vicinity of pyrroles I and II (Figure 1A). Methods to date have failed either to locate any propionate α-methylene signals or to identify the β-methylene signals with individual propionate side chains. The reconstitution of apocytochrome b_5 with hemin has demonstrated that there exists in solution an equilibrium involving two forms of the protein[15] which differ in the orientation of the heme.[20] Since the isomer with the X-ray determined orientation[10] dominates in solution,[18] we will concern ourselves here only with assignment and analysis of the major component peaks.

While direct application of NOEs to assign resonances has been largely restricted to diamagnetic proteins,[22–24] recent results on several systems have indicated that paramagnetic leakage is relatively minor and that NOEs should have the same powerful and general potential for effecting assignments in paramagnetic

(1) (a) University of California, Davis. (b) University of Bergen.
(2) Strittmatter, P.; Spatz, L.; Corcoran, D.; Rogers, M. J.; Setlow, B.; Redline, R. *Proc. Natl. Acad. Sci. U.S.A.* **1974**, *71*, 4565–4569.
(3) Hultquist, D. E.; Sannes, L. G.; Juckett, D. A. *Curr. Top. Cell. Regul.* **1984**, *24*, 287–300.
(4) Ito, A. J. *Biochemistry (Tokyo)* **1980**, *87*, 73–80.
(5) Hagler, L.; Coppes, R. I.; Herman, R. H. *J. Biol. Chem.* **1979**, *254*, 6505–6514.
(6) Livingston, D. J.; McLachlan, S. J.; La Mar, G. N.; Brown, W. D. *J. Biol. Chem.* **1985**, *260*, 15699–15707.
(7) Ozols, J. *J. Biol. Chem.* **1972**, *247*, 2242–2245.
(8) Slaughter, S. R.; Williams, C. H.; Hultquist, D. E. *Biochim. Biophys. Acta* **1982**, *705*, 228–237.
(9) Mathews, F. S.; Czerwinski, E. W.; Argos, P. "The Porphyrins"; Dolphin, D., Ed.; Academic: New York, 1979; Vol. 7, pp 107–147.
(10) Mathews, F. S. *Biochim. Biophys. Acta* **1980**, *622*, 375–379.
(11) Mauk, M. R.; Reid, L. S.; Mauk, A. G. *Biochemistry* **1982**, *21*, 1843–1846.
(12) Eley, C. G.; Moore, G. R. *Biochem. J.* **1983**, *215*, 11–21.
(13) Mauk, M. R.; Mauk, A. G. *Biochemistry* **1982**, *21*, 4730–4734.
(14) Reid, L. S.; Taniguchi, V. T.; Gray, H. B.; Mauk, A. G. *J. Am. Chem. Soc.* **1982**, *104*, 7516–7519.
(15) Keller, R. M.; Groudinsky, O.; Wuthrich, K. *Biochim. Biophys. Acta* **1976**, *427*, 497–511.
(16) Salemme, F. R. *J. Mol. Biol.* **1976**, *102*, 563–568.
(17) Poulos, T.; Mauk, A. G. *J. Biol. Chem.* **1983**, *258*, 7369–7373.
(18) Keller, R. M.; Wuthrich, K. *Biochim. Biophys. Acta* **1980**, *621*, 204–217.
(19) Wuthrich, K.; Keller, R. *Biol. Magn. Reson.* **1981**, *3*, 1–52.
(20) La Mar, G. N.; Burns, P. D.; Jackson, J. T.; Smith, K. M.; Langry, K. C.; Strittmatter, P. *J. Biol. Chem.* **1981**, *256*, 6075–6079.
(21) McLachlan, S. J.; Burns, P.; La Mar, G. N.; Strittmatter, P., manuscript in preparation.
(22) Noggle, J. H.; Shirmer, R. E. "The Nuclear Overhauser Effect"; Academic Press: New York, 1971.
(23) Dobson, C. M.; Olejniczak, E. T.; Poulsen, F. M.; Ratcliffe, R. G. *J. Magn. Reson.* **1982**, *48*, 97–110.
(24) Olejniczak, E. T.; Poulson, F. M.; Dobson, C. M. *J. Am. Chem. Soc.* **1982**, *103*, 6574–6580.

proteins, particularly in the presently relevant low-spin ferric state.[25-27] The NOE, η_{ij}, is defined as[22]

$$\eta_{ij} = \frac{I_j - I_{j0}}{I_j} \quad (1)$$

where I_j and I_{j0} are the intensity of proton j with and without saturating proton i. The time development of η_{ij} can be followed as a function of time that proton i is saturated and for a two-spin system is given by[23]

$$\eta_{ij}(t) = \frac{\sigma_{ij}(1 - e^{-\rho_j t})}{\rho_j} \quad (2)$$

where ρ_j is the intrinsic spin–lattice relaxation time of H_j and σ_{ij} is the cross-relaxation rate for H_i and H_j. In the applicable slow-motion limit, we have

$$\sigma_{ij} = \frac{-\hbar^2\gamma^4\tau_c}{10r_{ij}^6} \quad (3)$$

where τ_c is the protein tumbling time and r_{ij} is the interproton distance. In the limit of short irradiation times, eq 2 reduces to

$$\eta_{ij} = \sigma_{ij}t \quad (4)$$

also refered to the truncated NOE, which makes η_{ij} proportional to the inverse sixth power of the interproton distance. For long irradiation times, eq 2 simplifies to the generally used form, the steady-state NOE,

$$\eta_{ij} = \sigma_{ij}/\rho_j \quad (5)$$

Quantitative distance comparisons require the use of the truncated NOE to obtain σ. However, the more readily observed steady-state NOE can still qualitatively reflect relative distances if care is taken to ensure that the NOEs are primary.

We present herein the NOE-based assignments of individual propionate side chains for ferricytochrome b_5 and identify the 6-propionate as the titrating group which is capable of binding extrinsic metal ions and whose shifts are the most sensitive to complex formations with partner redox proteins. The observed hyperfine shifts suggest small but significant differences in propionate side chain orientations between solid state and solution, and variations in these shifts indicate a direct participation of the 6-propionate in an interprotein salt bridge.

Methods

The trypsin-resistant heme peptide of cytochrome b_5 was isolated from fresh bovine liver following the procedure of Mauk.[28] The protein had an A_{412}/A_{280} value of 5.8.

NMR samples consisted of a 3 mM solution of the protein in ^2H_2O; the pH of the solution was adjusted by the addition of small amounts of ^2HCl or NaO^2H and was measured using a Beckmann 3550 pH meter equipped with an Ingold combination microelectrode; pH values are not corrected for isotope effect.

Proton NMR spectra were collected using a Nicolet 500-MHz spectrometer operating in the quadrature mode. A typical spectrum consisted of ~1500 transients with a sweep width of 15 kHz and 8192 data points. Steady-state NOE experiments were carried out by saturating the resonance of interest for 300 ms with the decoupler. Difference spectra were taken by subtracting a reference spectrum, with the decoupler off resonance, collected under exactly the same conditions. The percentage NOE was calculated by measuring the area of each peak in the difference spectrum relative to the area of the saturated peak, also from the difference spectrum. The NOEs were reported on a per proton basis. An estimated error of 10–15% is found in measuring the NOEs.

Table I. Steady-State NOEs for Ferricytochrome b_5

	satd peak			
obsd peak	*B*	*E*	*F*	*R*
B (5-CH_3)		4%	3%	0
E (6-α-CH)	6%		56%	14%
F (6-α-CH)	4%	50%		14%
N (6-β-CH)	1%	17%	15%	51%
R (6-β-CH)	1%	13%	15%	

	satd peak			
obsd peak	C	S	W	X
C (7-α-CH)		32%	13%	15%
J (8-CH_3)	7%	8%	0	0
K (7-β-CH)	28%	25%	19%	45%
L (pro 40-β-CH)	18%	0	50%	27%
S (7-α-CH)	59%		8%	8%
W (pro 40-β-CH)	16%	6%		*a*
X (7-β-CH)	11%	7%	*a*	

[a] NOE cannot be calculated due to the peak overlap and spillage.

In the upfield region where the hyperfine shifted peaks are very crowded, power less than that required for complete saturation was used to avoid problems associated with spillage. The linearity of the percent NOE as a function of peak saturation was demonstrated by saturating peak S to varying degrees and observing the NOE to peak C. Peaks very close to peak S showed a nonlinear response indicating that spillage was present.

Truncated NOE experiments were carried out by selectively saturating the peak of interest for varying times, τ, ranging from 30 to 300 ms. Difference spectra were taken as described above.

$GdCl_3 \cdot 6H_2O$ was dissolved and recrystallized several times in ^2H_2O. A final solution of the 8 mM $GdCl_3 \cdot 6D_2O$ was prepared and the pH was adjusted to 5.5. Aliquots of the Gd solution were added to the cytochrome b_5 sample and the NMR spectrum was recorded as described above. The pH of the sample was maintained at pH 6.4.

Results

The hyperfine-shifted portions of the ^1H NMR spectrum of ferricytochrome b_5 are illustrated in B, C, and D of Figure 1. The set of resonances A–Z arise from the major component with the heme orientation as found in crystals. The smaller set of peaks, a–z (of which only a few are apparent) are due to the minor component.[20] We will be concerned here only with the major component since only for this species has the binding to potential redox proteins been described.[12,6] Since not all peaks are simultaneously resolved under one set of conditions, both temperature and pH variations are necessary. The temperature dependence for most peaks of interest has been reported previously.[29] The results of a pH titration over the stable range of the protein are presented in Figure 2; there is excellent agreement for those peaks for which previous pH data exist.[15] Most resonances exhibit essentially pH-independent shifts. Dramatic exceptions to this are peaks B, E, F, and R, which reflect a titrating group with a $pK \sim 5.9$. Much weaker, but similar, pH variations are noted for peaks S and, to a lesser extent, C and H. The heme methyls have been located and assigned 1-CH_3 (H), 3-CH_3 (G), 5-CH_3 (B), and 8-CH_3 (2.70 ppm; under protein envelope). The 2-vinyl group gives rise to peaks A (H_α), Y (H_β (cis)), and Z (H_β (trans)). Peaks R and X have been identified as arising from 6,7-propionate β-methylene protons.[21]

7-Propionate Assignment. Identification of the 7-propionate signals is initiated by saturating peak C in Figure 3, which yields a large (~50%) steady-state NOE to peak S and smaller ones for the resolved peaks W and X and peaks J, K, and L under the protein envelope. The results of a complete truncated NOE study upon saturating peak C are plotted in Figure 4; the solid line represents the fit to eq 2 with $\sigma_{cs} = -14\ s^{-1}$ and $\rho_s = 23\ s^{-1}$. The σ is quantitatively consistent (calculated $\sigma_{calcd} = -13.8\ s^{-1}$) with

(25) Ramaprasad, S.; Johnson, R. D.; La Mar, G. N. *J. Am. Chem. Soc.* **1984**, *106*, 5330–5335.
(26) Trewhella, J.; Wright, P. E.; Appleby, C. A. *Nature (London)* **1980**, *280*, 87–88.
(27) Moore, G. R.; Williams, G. *Biochim. Biophys. Acta* **1984**, *788*, 147–150.
(28) Reid, L. S.; Mauk, A. G. *J. Am. Chem. Soc.* **1982**, *104*, 841–845.
(29) Keller, R. M.; Wuthrich, K. *Biochim. Biophys. Acta* **1972**, *285*, 326–336.

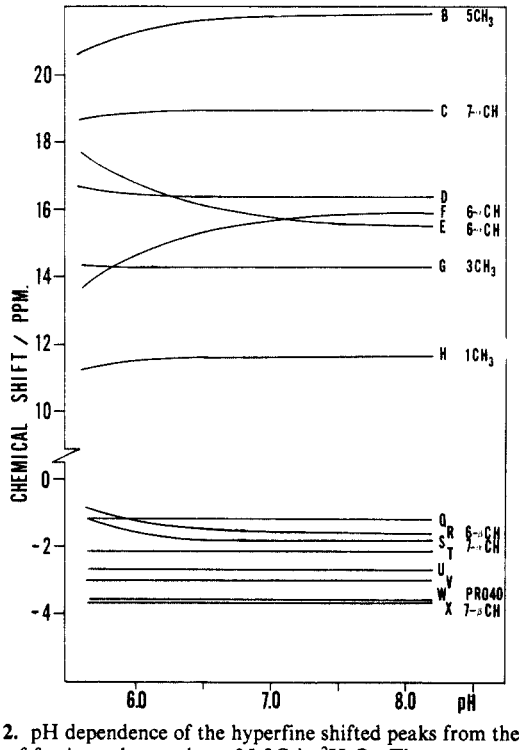

Figure 2. pH dependence of the hyperfine shifted peaks from the major species of ferricytochrome b_5 at 25 °C in ^2H_2O. The resonances from the 2-vinyl group (A, Y, and Z) are not shown.

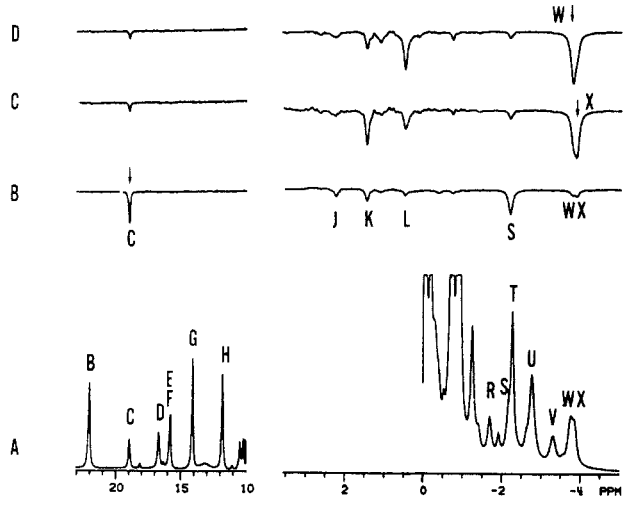

Figure 3. Portions of the downfield and upfield hyperfine shifted regions of the 500-MHz ^1H NMR spectrum of ferricytochrome b_5 in ^2H_2O at 20 °C and pH 6.75. The arrows indicate which peak is being saturated in each of the subsequent difference spectra: (A) reference spectrum; (B) steady-state NOE difference spectrum following saturation of peak C for 300 ms; (C) steady-state NOE difference spectrum following saturation of peak X for 300 ms; (D) steady-state NOE difference spectrum following saturation of peak W for 300 ms.

that expected for an immobilized ($\tau_c \sim 8$ ns) methylene group (r_{cs} = 1.77 Å). Thus such a large NOE is diagnostic of a methylene group in our protein.

Peak J seen in the difference NOE spectra upon saturating both C (Figure 3) and S (Figure 5) has the same shift as that reported for 8-CH_3 (2.70 ppm at 25 °C).[18] Saturating peak C at various temperatures reveals a very large temperature dependence (0.09 ppm/°C) for J which is consistent with the near cancellation of upfield dipolar (T^{-2}) and downfield contact (T^{-1}) contributions[30] to the near-zero 8-CH_3 hyperfine shift at 25 °C. Thus C and S

(30) Jesson, J. P. In "NMR of Paramagnetic Molecules"; La Mar, G. N., Horrocks, W. D.; Holm, R. H., Eds.; Academic Press: New York, 1973; pp 1-51.

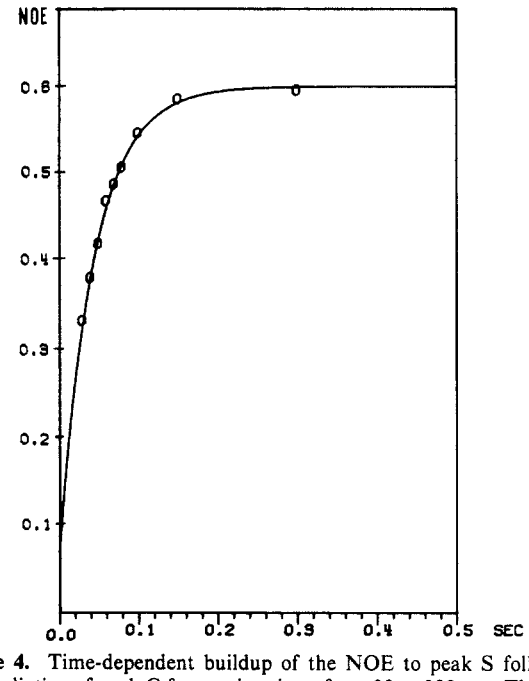

Figure 4. Time-dependent buildup of the NOE to peak S following preirradiation of peak C for varying times from 30 to 300 ms. The solid line represents a fit of the data using eq 2. The fit yields a cross-relaxation rate σ_{CS} = 14 s^{-1} and intrinsic relaxation rate ρ_S = 23 s^{-1}.

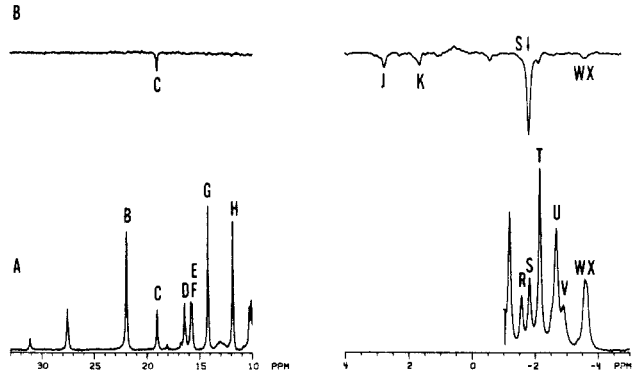

Figure 5. Hyperfine shifted region of the 500-MHz ^1H NMR spectrum of ferricytochrome b_5 at 25 °C and pH 6.80 in ^2H_2O; under these conditions peak S is better resolved from peak T: (A) reference spectrum; (B) steady-state NOE difference spectrum following saturation of peak S for 300 ms.

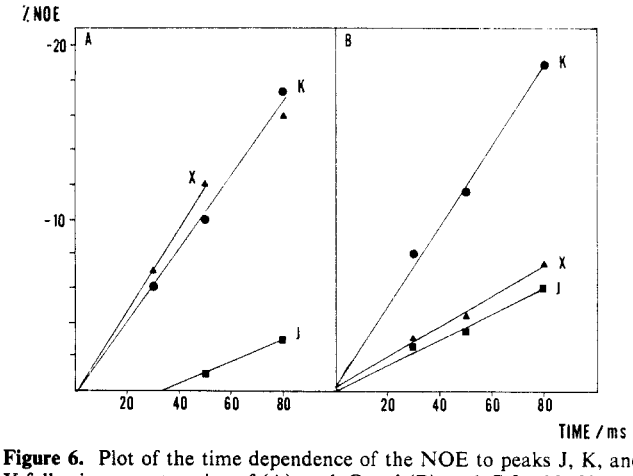

Figure 6. Plot of the time dependence of the NOE to peaks J, K, and X following presaturation of (A) peak C and (B) peak S for 30, 50, and 80 ms. The line joining the points does not represent any fit to the data. At longer saturation times the NOE is no longer linear in time (eq 4) and some curvature becomes apparent.

are geminal protons in the close proximity of both 8-CH_3 (J) and a propionate β-CH (peak X) and hence must arise from 7-α-CH_2.

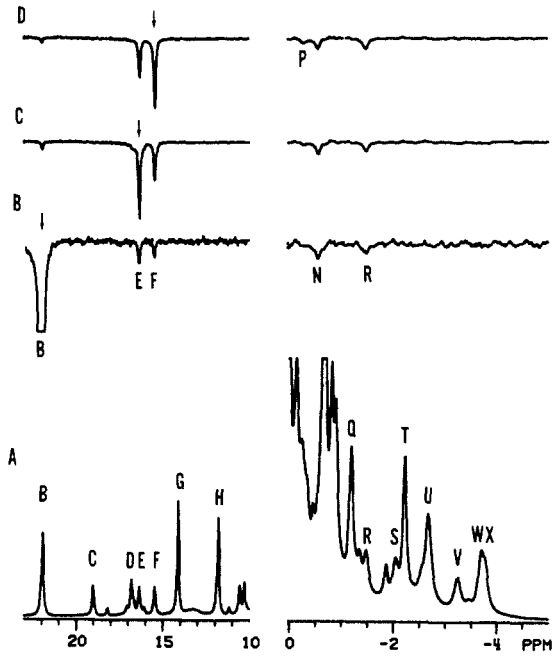

Figure 7. Portions of the hyperfine shifted region of ferricytochrome b_5 in ^2H_2O at 20 °C and pH 6.20: (A) reference spectrum; (B–D) steady-state NOE difference spectra following saturation of peaks B, E, and F.

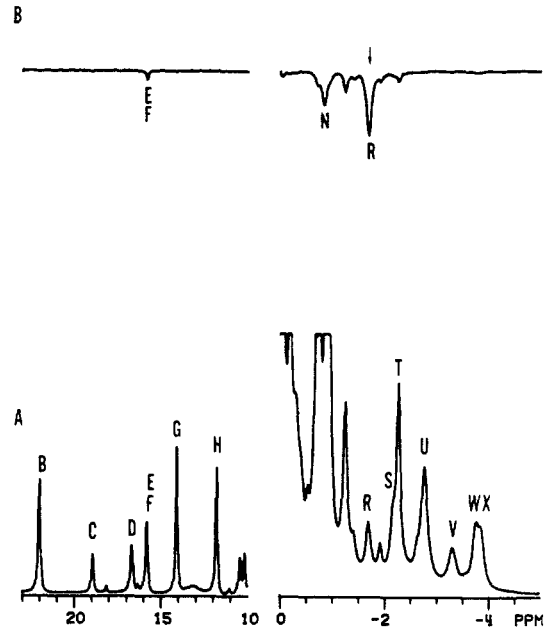

Figure 8. Portions of the hyperfine shifted regions of the ^1H NMR spectrum of ferricytochrome b_5 in ^2H_2O at pH 6.75 and 20 °C. These conditions best resolve peak R: (A) reference spectrum; (B) steady-state NOE difference spectrum following saturation of peak R for 300 ms.

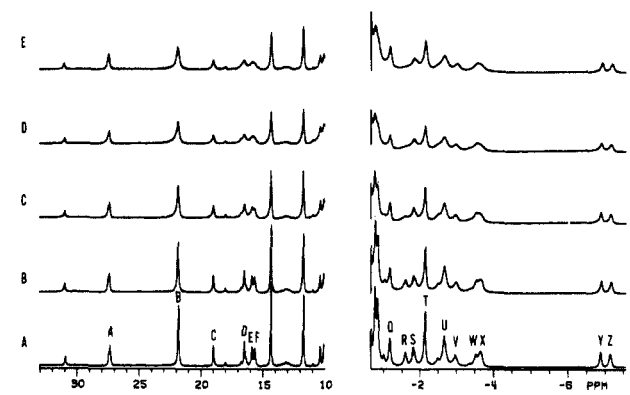

Figure 9. Upfield and downfield portions of the hyperfine shifted spectrum of a 1 mM solution of ferricytochrome b_5 in ^2H_2O at pH 6.4 and 25 °C with varying mole ratios of Gd^{3+}/cytochrome b_5: (A) 0.0; (B) 0.7; (C) 0.14; (D) 0.21; (E) 0.28.

The time dependence of the NOEs at short saturating times resulting from saturating peaks C and S are plotted in A and B of Figure 6, respectively. All NOEs extrapolate to the origin at zero time except for peak J when saturating C. This establishes that S is very close to 8-CH_3 (J) and that C yields a steady-state NOE via a secondary effect due to the very strong C,S cross relaxation. The data in Figure 6 similarly establishes that $\sigma_{CK} \sim \sigma_{SK}$ (and hence $r_{CK} \sim r_{SK}$) and that $\sigma_{CK} \sim \sigma_{CX} > \sigma_{SX}$, which places C similarly close to both K and X and X closer to C than S.

Saturating X (a propionate β-CH) yields a large (~50%) NOE to peak K (Figure 3C), as well as smaller NOEs to peaks C and S. Thus X and K are geminal partners of a propionate β-methylene group and the NOE to C and S assign it to the 7-β-CH_2. The NOE to peak L is traced to partial saturation of the partially overlapping peak W. Thus C, S and X, K comprise the 7-propionate α- and β-methylene protons, respectively.

Centering the decoupler on peak W (Figure 3D) leads to a large (~50%) NOE to L, established W,L as geminal partners of a methylene group *not arising from a propionate* but in the vicinity of pyrrole IV. The NOEs from W to 7-α-CH_2 (C,S) but not 8-CH_3 (J) indicate W,L arises from the β-CH_2 of proline 40. Several other small NOE's in Figures 3 and 5 suggest additional peaks from proline 40. Our inability in effecting selective saturation of these peaks precludes further assignments pending the extension of 2D NOE methodology[31] to paramagnetic systems. The exploration of such methodology is in progress.

6-Propionate Assignment. Saturation of the assigned 5-CH_3 (B) peak (Figure 7) gives rise to negative NOEs to four hyperfine shifted resonances, the resolved peaks E, F, and *R* and an unresolved peak at −0.5 ppm labeled N (Figure 7B). At short saturation times the NOE to peak E is larger than for peak F (not shown). Saturation of peak E (Figure 7C) or F (Figure 7D) leads to a ~50% NOE between E and F and NOEs to peak R and N. Again, at short saturating times, the NOE from E to B is larger than from F to B. Thus E,F comprises the 6-propionate α-methylene group, with E oriented closer to 5-CH_3. The NOE from E and F to R establishes the latter as a 6 β-propionate methylene proton. (The fact that the two propionate β-methylene proton identified by isotope labeling originate in different propionate side chains is evidenced by the complete absence of an NOE between peak X and R). An additional weak peak P noted in the difference NOE spectra when saturating E or F (Figures 7C,D) is consistent with arising from either a γ-meso-H or a Gly 41 α-proton; these assignments could be established if planned 2D NOE studies are successful.

The location of the geminal partner to R requires a higher pH where R is better resolved, as shown in A of Figure 8; under these conditions peaks E and F are coincident. Saturating R shows a large NOE (>40%) to peak N which confirms that N and R are the geminal partners of the 6-propionate β-methylene group. It may be noted that peak N yields (of peaks N,R) the larger NOE when E is saturated (Figure 7C); the reverse is observed when F is saturated (Figure 7D). Thus N is closer to E than F and R is closer to F than E. This completes the location of the 6-propionate signals.

Gd^{3+} Binding to Heme Propionates. The influence of incremental addition of Gd^{3+} to a ferricytochrome b_5 solution at pH 6.4 is illustrated in Figure 9. The most dramatic effect is the broadening[32] of the β-methylene proton peak R from the 6-propionate, while the analogous peak for the 7-propionate (peak

(31) Wider, G.; Macura, S.; Kumar, A.; Ernst, R. R.; Wuthrich, K. *J. Magn. Reson.* **1984**, *56*, 207–234.

(32) Inagaki, F.; Miyazawa, T. *Prog. Nucl. Magn. Reson. Spectrosc.* **1981**, *14*, 67–111.

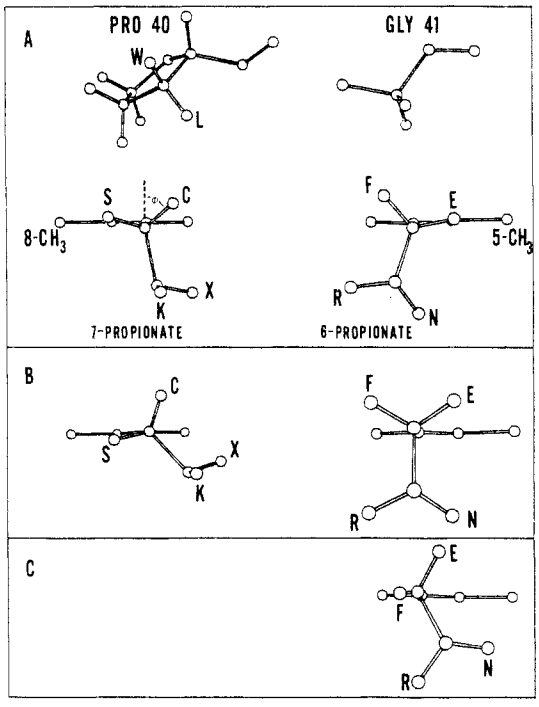

Figure 10. Projection of the heme propionate group relative to the heme plane at both 6- and 7-positions. The view shown is looking directly down the C_α–C_π bond for each propionate. The carboxyl group of each propionate is omitted for clarity. (A) The crystallographic-determined orientation of the heme propionate groups at positions 6 and 7.[10,33] The NOE experiments have lead to the stereospecific assignment of the four methylene groups on the heme propionates as shown in the figure. B) The revised orientation of the heme propionate groups at pH 8 based on the NMR experiments. The heme 7-propionate has been rotated counterclockwise by 30° about the pyrolle carbon α-carbon bond relative to the crystallographically defined orientation. The heme 6-propionate has also been rotated in a similar manner so that protons E and F are more symmetrically oriented relative to the heme plane. (C) The orientation of the heme 6-propionate group upon protonation at low pH; the NMR results predict peak E moves more out of the plane of the heme group as the pH is lowered. The 7-propionate group does not titrate.

X) is essentially unaffected. The selective binding of Gd^{3+} to the 6-propionate is confirmed by the simultaneous but lesser (due to r^{-6} (Gd–H) dependence) broadening of peaks E and F (6-propionate α-CH_2) and that for the 5-CH_3 (B) but not of peaks C and S (7-propionate α-CH_2).

A more quantitative analysis of the Gd^{3+}-induced relaxation on the basis of relative distances is complicated by both spectral overlap and the fact that there are several other possible acidic binding sites on the protein surface. However, the lack of any other surface acidic residues close to the exposed pyrrole ring and the relatively selective perturbation of resonances on pyrrole III indicate that Gd^{3+} is binding to an exposed heme carboxyl group associated with the 6-propionate.

Discussion

Propionate Assignments. The orientation of the two propionate side chains, as determined from available X-ray coordinates,[10,33] are depicted in A of Figure 10. The carboxylate of the 6-propionate is found exposed to solvent, while the 7-propionate group is buried, with its carboxylate hydrogen-bonded to serine 64. The larger NOE from 5-CH_3 to E than F identifies E as the diastereotopic methylene proton closer to the methyl. Similarly, the relative magnitudes of the NOE from E and F to N and R dictate N is closer to E and R is closer to F, as illustrated on the right-hand side of Figure 10A. For the 7-propionate, the larger NOE to 8-CH_3 (J) from S than C places S closer to 8-CH_3. Moreover, the similar NOE from both C and S to K identifies K as the β-methylene pointing forward, as depicted in the left-hand side of Figure 10A. Thus the relative NOEs are qualitatively consistent with the propionate orientations, particularly as described by the C_α–C_β rotations.

(33) Mathews, F. S., private communication.

Table II. Pyrrole Ring III and IV Substituent Chemical Shift in ppm at 25 °C

	pH				
peak	4.0[a]	6.0	8.5[b]	5.6	5.6[c]
B (5-CH_3)	20.15	21.16	21.81	20.49	20.73
E (6-α-CH)	18.58	16.75	15.52	17.78	17.33
F (6-α-CH)	12.70	14.52	15.90	13.35	13.86
R (6-β-CH)	−0.56	−1.10	−1.64	*d*	*d*
N (6-β-CH)		−0.57[e]			
C (7-α-CH)		18.80	19.0		
S (7-α-CH)		−1.60	−1.80		
X (7-β-CH)		−3.60	−3.65		
K (7-β-CH)		1.62[e]			
J (8-CH_3)		2.76[e]			

[a] Calculated for protonated 6-propionate on the basis of pK of 5.9. [b] Observed shifts for the 6- and 7-propionates ionized. [c] Cytochrome b_5 with 1 equiv of bovine metmyoglobin. [d] Peak R is unresolved at pH 5.6. [e] Calculated from NOE spectrum at pH 6.4.

It is also obvious from Figure 10A that proline 40 is the prime candidate for NOEs from 7-α-CH_2 and that glycine 41 may be the origin of the additional NOEs from 6-α-CH_2. As indicated above, confirmation of the amino acid assignments as well as interpretation of other NOEs must await the results of planned 2D NOESY experiments. The detection of only primary NOEs, except when saturating a peak coupled to a tightly coupled methylene pair, indicates that there is negligible spin diffusion.[34] The sizable NOEs, only slightly reduced by paramagnetic leakage from those observed for analogous diamagnetic systems, demonstrates the broad scope of NOE-based assignments in paramagnetic proteins. Our recent observation of interpretable NOEs in high-spin ferric myoglobin[35] also makes clear that useful NOE studies are not restricted to systems with only weak paramagnetism.

The pH behavior of the two propionates (Figure 2) thus identifies the 6-propionate as the titrating group and the side chain that can bind extrinsic metal ions. The very slight pH behavior of peak S is not due to titration of the 7-propionate but rather represents a small perturbation of the titration of the neighboring 6-propionate group. Consistent with this, it is noted that the other resolved 7-propionate signals C and X exhibit essentially pH-independent shifts. Assuming that both propionates are ionized at pH 8.5, we obtain the chemical shifts for the two side chains at pH 8.5 and 6.0 and estimate the shifts for the 6-propionate in the protonated forms at pH 4.0 on the basis of the pK ~ 5.9 in Figure 2; the chemical shifts are listed in Table II.

Heme Propionate Orientation. An interesting contrast between the two propionates for the neutral-to-alkaline pH form of the protein is the near identity of the two 6-α-methylene hyperfine shifts, while the two 7-α-methylene protons exhibit widely different hyperfine shifts, with C very far downfield and S slightly upfield of their normal diamagnetic position near 3.5 ppm.

The origin of the hyperfine shifts is a combination of the dipolar and contact contribution.[30] The relevent dipolar shift has the form

$$(\Delta H/H)^{dip} = (1/2R^3)[(\chi_{zz} - \bar{\chi})(3\cos^2\theta - 1) + (\chi_{xx} - \chi_{yy})\sin^2\theta\cos 2\Omega] \quad (6)$$

where θ and Ω are the polar and azimuthal angles in the magnetic coordinate system described by the susceptibility tensor χ_{xx}, χ_{yy}, χ_{zz}, and R is the iron–proton distance. For the present system, neither the individual χ_{ii}s nor the location of the magnetic axes are known. However, since the magnetic anisotropy in low-spin ferric systems does not exceed $^1/_2\bar{\chi}$, and R is essentially the same for two α-methylene protons, the H–Fe–H angle of ~16° allows

(34) Kalk, A.; Berendsen, H. J. C. *J. Magn. Reson.* **1976**, *24*, 343–366.
(35) Unger, S. W.; Lecomte, J. T. J.; La Mar, G. N. *J. Magn. Reson.* **1985**, *64*, 343–366.

a maximum of ~5 ppm difference in the two methylene protons due to magnetic anisotropy. Thus, the difference of ~20 ppm for 7-α-CH_2 must originate in the scalar contact shift.

This scalar contribution to the hyperfine shift is given by[36]

$$(\Delta H/H)^{con} = -(A/\hbar)K/T \quad (7)$$

where $A/\hbar$ is the ferric coupling constant and K is a constant for the particular system. For a methylene group directly attached to a π radical, $A/\hbar$ takes the form

$$(A/\hbar)^{CH_2} = Q_0 + Q_2 \cos^2 \phi \quad (8)$$

where Q_2 is a negative constant, Q_0 is close to zero, and ϕ is the dihedral angle between the methylene C_π–C_α–H plane and the pyrrole $C_\pi P_z$ axis. Thus different shifts for two methylene protons represent nonsymmetrical positions of the two protons about the heme normal through C_π.

Therefore, the 7-α-CH_2 +20 and −2 ppm shifts are inconsistent with the X-ray determined ϕ_C ~50° and ϕ_S ~−70°, which predict only a ~30% difference in hyperfine shifts. The experimental shifts, in fact, indicate that S is nearly in plane or that the methylene group is rotated some 30–40° counterclockwise from that found in the crystal, as depicted schematically in B of Figure 10. This accounts both for the large C and the negligible S contact shifts. This difference in solution and crystal α-propionate orientation may, in fact, not represent a true difference. In fitting the electron density maps, Mathews et al.[9] experienced considerable difficulties in the vicinity of pyrrole IV and optimized the fit by somewhat arbitrarily buckling the pyrrole π plane. Thus the X-ray coordinate determined orientation may, in part, represent an artifact of the fitting procedure.

For the 6-propionate α-CH_2, the X-ray coordinates yield ϕ_F ~−40° and ϕ_E ~80°, predicting ~50% difference in shifts, while the observed shifts for E and F are essentially the same for the deprotonated carboxylate. Thus the NMR shifts suggest a more symmetrical environment for E and F, as schematically illustrated in B of Figure 10.

The protonation of the 6-propionate carboxylate, as indicated by the pK reflected in the hyperfine shifts for the 6-propionate and the 5-CH_3 signals, results in the generation of a large difference in the E and F contact shifts. The ~50% larger hyperfine shift for E when compared to F predicted for the fully protonated group (Table II) suggests that F is much more in plane than for the ionized group or that protonation results in a rotation of the 6-α-CH_2 ~20° counterclockwise, as schematically represented in C of Figure 10. The lack of a quantitative model for interpreting β-methylene contact coupling constants precludes an interpretation of the nature of any changes in the C_α–C_β rotational angle in either propionate.

The Nature of Heme Propionate Interaction in Protein Complexes. The NOE assignments clearly demonstrate that it is the 6-propionate group (and the 5-CH_3) that are selectively perturbed upon complex formation between ferricytochrome b_5 and either cytochrome c[12] or myoglobin.[6] This is, as had been speculated, the same group found extended to the protein exterior in the crystal structure. The selective binding of Gd^{3+} to the 6-propionate carboxyl group confirms that this group is also exposed to solvent in solution. The direct participation of the 6-propionate carboxyl group in forming a salt bridge with a positively charged side chain in the partner protein has been proposed for the 1:1 complexes with cytochrome c,[16] hemoglobin,[17] and myoglobin,[37] based on computer "docking" on the basis of charge complementarity.

The selective perturbation of the functional group attached to pyrrole III upon complex formation could arise from several distinct origins, the most likely being a simple rotation of the propionate side chain or the change in the pK of the carboxylate, or both. It is observed (see Table II) that the spectral perturbations on binding myoglobin,[6] for example, affect primarily peaks B, E, and F and induce shifts of the same relative magnitudes and in the same direction as by simply raising the pH of the pure protein solution by 0.4 units.

Thus complex formation induces shifts for the pyrrole III substituents which behave as if the pK of the propionate carboxylate were lowered by 0.4 units in the 1:1 complex. The instability of the 1:1 complex with Mb over an extended pH range unfortunately prevents an experimental verification of this interpretation. The lowering of the pK is in contrast to the expected raising of the pK that may be anticipated if the carboxylate were simply transferred into a solvent-excluded hydrophobic interface between the two proteins. This decrease in the pK, however, is consistent with expectation if the exposed 6-propionate carboxylate directly interacted with a positively charged amino acid side chain on the partner protein, as predicted to be the case in both complexes.[16,17]

Further information on the detailed solution conformation of ferricytochrome b_5 and the nature of its interaction with partner redox protein is dependent on additional resonance assignments which are currently being explored by two-dimensional NMR methods.

Acknowledgment. We are indebted to A. G. Mauk and J. T. Jackson for useful discussions, to A. G. Mauk for a gift of some cytochrome b_5, to E. Sletten, to P. Strittmatter for the original gift of cytochrome b_5 which stimulated the present work, and to F. S. Mathews for providing a set of X-ray corodinates. This research was supported by grants from the National Science Foundation, CHE-84-15329, and the Scientific Affairs Division of NATO, 1250.

(36) La Mar, G. N. In "NMR of Paramagnetic Molecules"; La Mar, G. N., Horrocks, W. D.; Holm, R. H., Eds.; Academic Press: New York, 1973; pp 85–126.

(37) Livingston, D. J.; McLachlan, S. J.; La Mar, G. N., unpublished results.